EVLA Memo 109
Wideband Performance of the EVLA L-Band System

Rick Perley and Bob Hayward
NRAO

February 14, 2007

Abstract

The performance of the EVLA L-band feed/receiver across its full 1.0 – 2.0 GHz range is presented. The median efficiency across the band is near 45%, rising by about 4% near 1300 MHz and 2000 MHz, and dropping by a similar value near 1600 MHz. The efficiency drops quickly below 1100 MHz. The variation of focus position with frequency follows predicted values, and an optimum position for wide-band observations causes less than 2% loss in efficiency at any frequency. The increase in system temperature with decreasing elevation is nearly independent of frequency.

1 Introduction

In EVLA Memo 85 (November 1994), we presented early tests of the EVLA L-band performance on antenna 13. These measurements were made with the new EVLA L-band horn, but retaining the VLA orthogonal mode transducer (OMT) and receiver, thus limiting accurate measurements to the 1300 – 1700 MHz band. The observations were made at the output of the receiver at four frequencies selected by the availability of RF filters: 1325, 1425, 1675, and 1975 MHz. For the highest of these, the gain of the VLA L-band receiver was so low that the quality of the derived results was severely degraded.

There are now eight EVLA antennas outfitted at L-band – seven with the 'interim receivers' providing full sensitivity and tuning capability between 1200 and 2000 MHz, and one – antenna 14 – outfitted with the prototype OMT, providing full tuning across the full 1.0 – 2.0 GHz band. In addition, we now have a powerful new investigative tool available for measurements of the frequency dependency of system characteristics – the 8-bit, 2 GSamp/sec digital data stream sampled at the antenna can be Fourier transformed and averaged to provide a convenient and useful measure of the spectral power density with a resolution as high as 250 kHz.

The availability of the new OMT, the full electronics system, and the full spectrum via the FFT now permits a proper 'end-to-end' test of the EVLA's L-band performance. In this memo, we report on system temperature, efficiency, subreflector focus position, and spillover, all as a function of frequency, for two antennas – #14, which has the new OMT, and #24, selected because it shows superior sensitivity from interferometric tests.

These tests did not enable determination of the system polarimetric characteristics. These will be reported in a later memo, following implementation of a second OMT on the array.

2 Observations

The observations performed are the same as reported in our preceding antenna memos:

- A hot load, consisting of a layer 3"-deep RF absorber, a 1"-thick carbon impregnated Zotefoam, topped with metal 'shorting plate' was placed over the feed, and the power spectrum taken. The temperature of the hot absorber was measured with a thermometer.
- A cold load power spectrum was taken. Ideally, the cold load would consist of a liquid nitrogen cooled absorber placed over the feed. This is not practical for the 2-meter aperture of the L-band horn, so we utilized the cold sky.
- An observation of the calibrator source 3C405 (Cygnus A) was taken, along with a nearby reference position, to determine the antenna efficiency.
- While tracking the calibrator, the subreflector was moved over a modest range to enable determination of the optimum focus position as a function of frequency.
- To determine the variation of system temperature with elevation, a 'sky dip' was made, and power spectra recorded for a set of fiducial elevations.

These observation were sufficient to enable determination of the system sensitivity, system temperature, antenna focus and efficiency, as functions of elevation and frequency.

Most observations were taken using the new FFT power spectrum analyzer[1]. The program grabs a short interval of the sampled data stream, performs a Fourier transform, and makes the spectrum (expressed either in linear or decibel power) available for plotting or writing to disk for subsequent analysis. From 128 to 4096 channels (corresponding to 16 to 0.25 MHz spectral resolution) can be selected, and from 2 to 2000 spectra can be summed. The sensitivity of this method is not high – a 4096 channel spectrum over the 1 GHz bandwidth uses only 4 microseconds of data. We utilized a 500-spectrum average, giving 2 milliseconds of integration – which provides a power variation of $\sim 5\%$ (rms) in the measurement of system spectral power.

These observations were taken on 04Dec2006, 11Dec2006, and 15Dec2006, all on IF 'A' – the RCP channel of the first IF pair.

2.1 Calibration

We utilized the same calibration methodology described in EVLA Memo #85, using hot and cold loads to calibrate the system gain and receiver temperature.

Presuming linearity and zero offset, the relationship between the measured output power P and the input power as characterized by the noise-equivalent temperature T is simply:

$$P = GkT\Delta\nu = KT \tag{1}$$

where G is the system gain, and $K = Gk\Delta\nu$ is a constant which absorbs the resolution bandwidth and Boltzmann's constant.

The calibration constant K is found from

$$K = \frac{P_h - P_c}{T_h - T_c}. \tag{2}$$

where the subscripts h and c denote the measured hot and cold powers and input temperatures. The noise-equivalent system temperature is then obtained by division of the observed power by this conversion constant: $T = P/K$.

[1]This is available at: https://webtest.aoc.nrao.edu/cgi-bin/wbrisken/bp1.cgi.

3 Results

3.1 Analog and Digital Results Comparison

We first measured the system 'Y-factor' between hot and cold loads, using an analog detection system, and the digital system. Confidence in the FFT spectral power data will be gained if the results are similar. These data were taken on 04Dec and 11Dec.

The analog measurements were taken with the arrangement shown in Figure 1. The power from the front-end was bandpass filtered (1425/60 MHz), amplified, detected, and recorded on a PC.

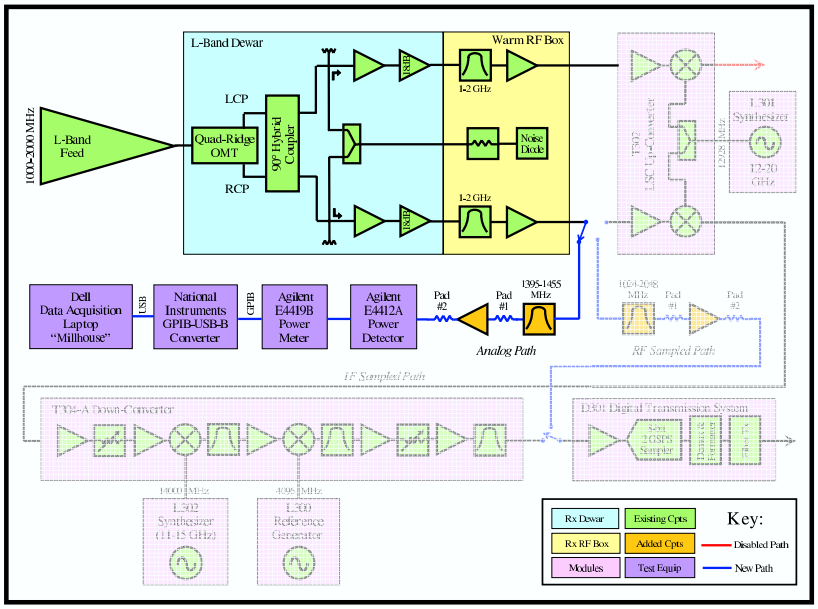

Figure 1: The setup for analog power measures, shown by the bold-tinted boxes. The RF output is bandpass filtered, amplified, and detected by the Agilent E4412A power detector, managed by the Agilent E4419B power meter, and recorded on a laptop via a GPIB-USB-B converter.

The digital sampling was done both at the RF and at the output of the IF, as we wished to measure the degradation in system performace due to the IF signal conversion. For the RF sampling, the setup is as shown in Figure 2. Here, the front-end output is bandpass filtered (1536/1024 MHz) to prevent aliasing, amplified, and sampled by the 2048 GSamp/sec DTS.

The setup for the IF measures is shown in Figure 3. Here, the signal traverses the full IF conversion and amplification path before sampling by the DTS.

A comparison of the sensitivities is best done directly from the 'Y-factor' – the ratio of the power detected between the hot load and the cold sky – as this quantity is independent of the calibration. A table of the results is shown in Table 1.

Date	Method	Y-Factor
04Dec	Analog	10.00 dB
04Dec	IF Samp	9.86
11Dec	Analog	9.37
11Dec	RF Samp	9.78
11Dec	IF Samp	9.29

Table 1: The Y-Factors between a hot load and cold sky, for antenna 14A.

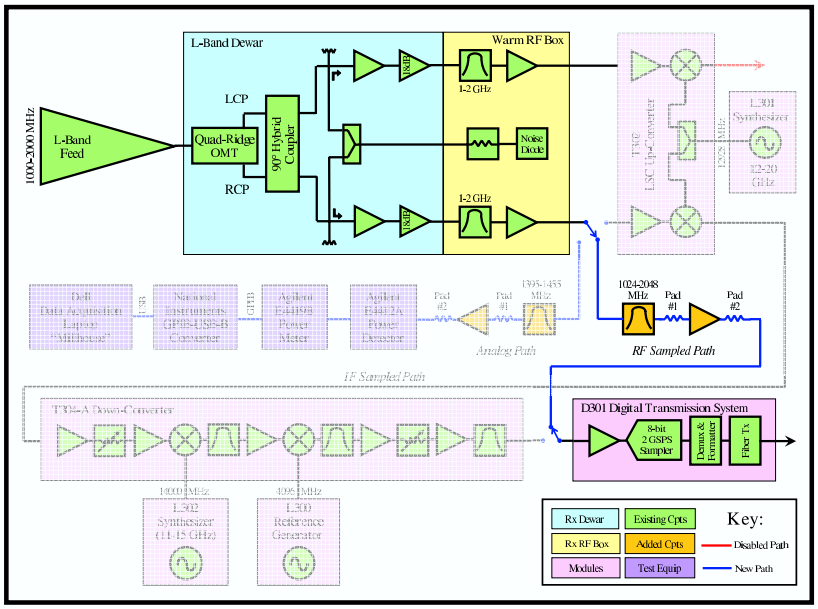

Figure 2: The setup for RF spectral power measures, utilizing the EVLA DTS system. In this arrangement, the RF output is bandpass filtered by a 1024-2048 MHz filter to prevent aliasing, amplified, and sampled by the 2.048 GSamp/sec DTS sampler. An off-line Fourier transform converts the time-ordered stream into the power spectrum.

The various Y-factor results are very similar, but the difference of about 0.6 dB between the two days is unexpected as the hot load temperatures were measured to be the same to within 3K on the two days. The drop in Y-factor must be due to a change in cold load temperature of about 5K – an increase in system temperature, spillover, or sky emission. It is not possible to discriminate between these without a true cold load observation.

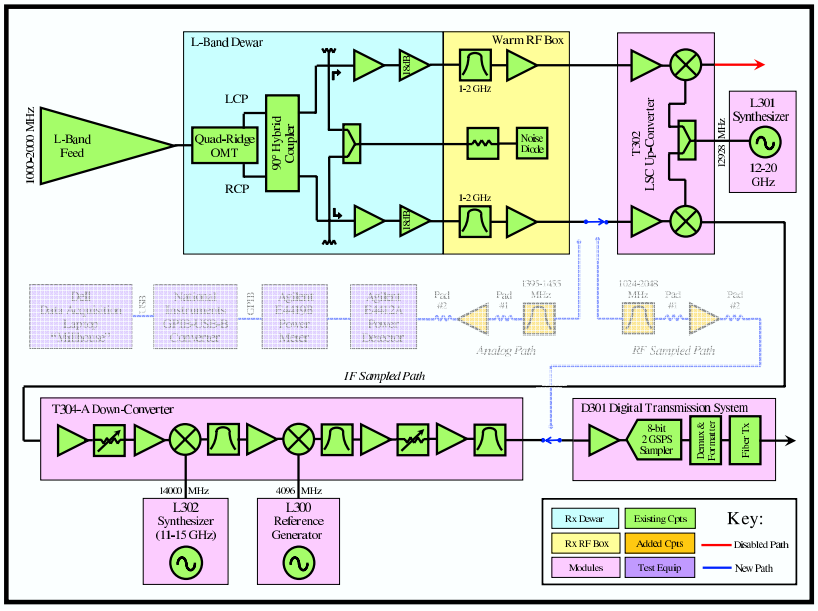

Figure 3: The setup for IF spectral power measures, utilizing the EVLA DTS system. In this arrangement, the signal path must traverse much more hardware, with some inevitable degradation – about 3K for antenna 14A.

Despite these unexplained differences, we are satisfied that the spectral technique gives a good measure of system performance.

3.2 System Sensitivity Loss due to IF Conversion

The difference between the RF sampled and IF sampled Y-factors on 11Dec provide evidence that the IF system for antenna 14A is introducing about a 0.4dB additional noise figure – equivalent to about 3K in noise temperature. The degradation is about the same across the entire spectrum, as shown in Figure 4, which shows the frequency dependence of the Y-factor for antennas 14 and 24. The dramatic narrow-band dips in Y-factor seen for both antennas are due to RFI, which affects only the cold sky observations. The differing sensitivities between the two antennas is discussed in the following section.

The dramatic oscillations in Y-factor for antenna 24 seen below 1300 MHz are due to the waveguide cutoff in its (old-style) VLA OMT. We discuss the frequency dependence of system sensitivity in the following section.

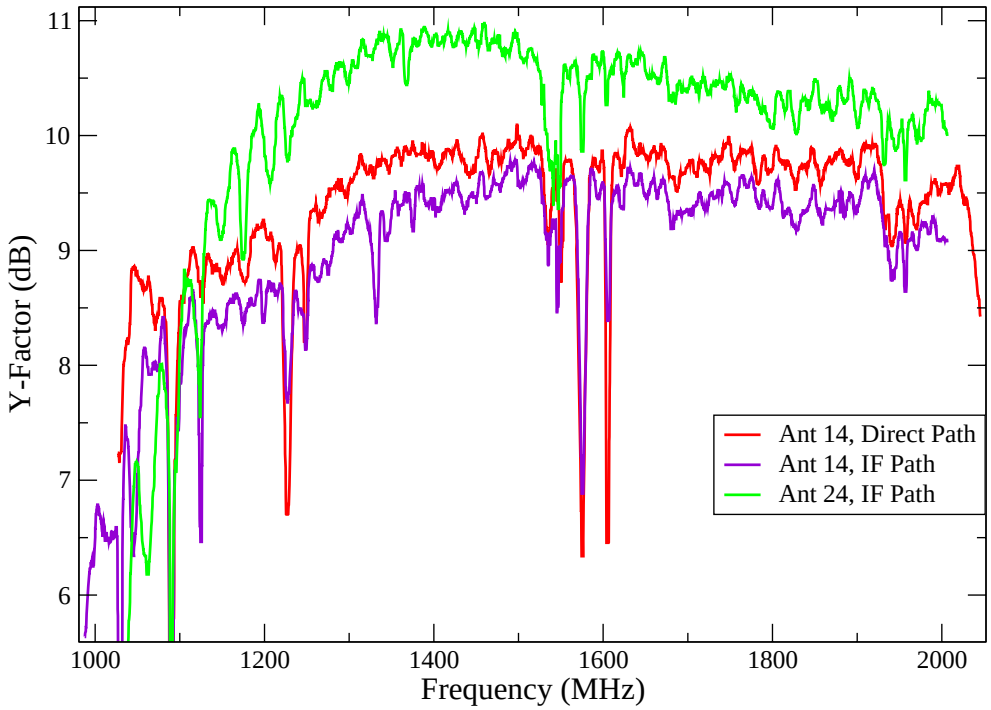

Figure 4: The observed Y-Factors for Antennas 14A and 24A are shown as functions of frequency. The large narrow bandwidth drops seen for both antennas are due to external interference, as the RFI is seen only in the cold sky observation. There is clear evidence the IF system in antenna 14A is reducing the Y-factor by about 0.4 dB across the entire band.

3.3 System Sensitivity

A very useful metric for antenna sensitivity is the 'System Equivalent Flux Density', often denoted as SEFD, defined as the spectral flux density of a source which doubles the system temperature. This quantity is determined by observing the power increment provided by a source of known flux density, and is independent of the calibration of the power detector, provided the response is linear over the range employed. The SEFD is related to the antenna efficiency and system temperature

by

$$\frac{\epsilon}{T_{sys}} = \frac{2k}{A_p}\frac{1}{SEFD} \tag{3}$$

where A_p is the antenna's physical aperture, and the SEFD is expressed in MKS units: $\mathrm{Wm^{-2}Hz^{-1}}$. The SEFD is normally expressed in units of Jy, in which case we have, for the EVLA antennas,

$$\frac{\epsilon}{T_{sys}} = \frac{5.62}{SEFD}. \tag{4}$$

A simple analysis shows that

$$SEFD = S_{cal}\frac{P_c}{P_{cal} - P_{ref}} \sim \frac{S_{cal}}{Y_l - 1} \tag{5}$$

where S_{cal} is the spectral flux density of the calibrator source, P_c is the spectral power measured on cold sky, P_{cal} is the power measured while on source, and P_{ref} is the spectral power when on a reference region. The approximation shown above applies when the power from the reference region is the same as the cold-sky (normally a good approximation if the observations are not taken at low elevations), and Y_l is the *l*inear power ratio between the calibrator and cold sky.

For EVLA antenna 14A, the SEFD at 1425 MHz is given in Table 2, from each of the days.

Date	Method	SEFD Jy
04Dec	Analog	412
04Dec	IF Samp	409
11Dec	IF Samp	430
15Dec	Direct	425
15Dec	IF Samp	450

Table 2: System Equivalent Flux Density for antenna 14A

The increase between Dec 4 and Dec 11 reflects the change in Y-factor between those days, as reported in the previous section.

By comparison, antenna 24A's SEFD was found to be 280 Jy on 11 Dec – a greatly better value, and confirms the results from interferometric measures that antenna 24A is considerably more sensitive than antenna 14A.

The dependence of the SEFD on frequency is shown in Figure 5. This shows that both antennas have their best sensitivity between 1200 and 1400 MHz, a modest degradation with increasing frequency to 1700 or 1800 MHz, and improving sensitivity at higher frequencies. The origin of the 'bump' above 1920 MHz is unknown, but there is some evidence for this also in interferometric measurements.

The improvement in sensitivity due to the new wide-band OMT is clearly evident at frequencies below 1200 MHz for antenna 14. The 15 MHz oscillatory pattern clearly visible in both antennas is due to a standing wave caused by a small return loss near the transition between the feed and receiver.

3.4 Cold Sky System Temperature and Antenna Efficiency

Calibration via hot and cold loads of known thermodynamic temperature permit separate determination of the antenna system temperature and its efficiency.

The results for antenna 14A, for both the 'RF Sampled' and 'IF Sampled' data streams, are shown in Figure 6.

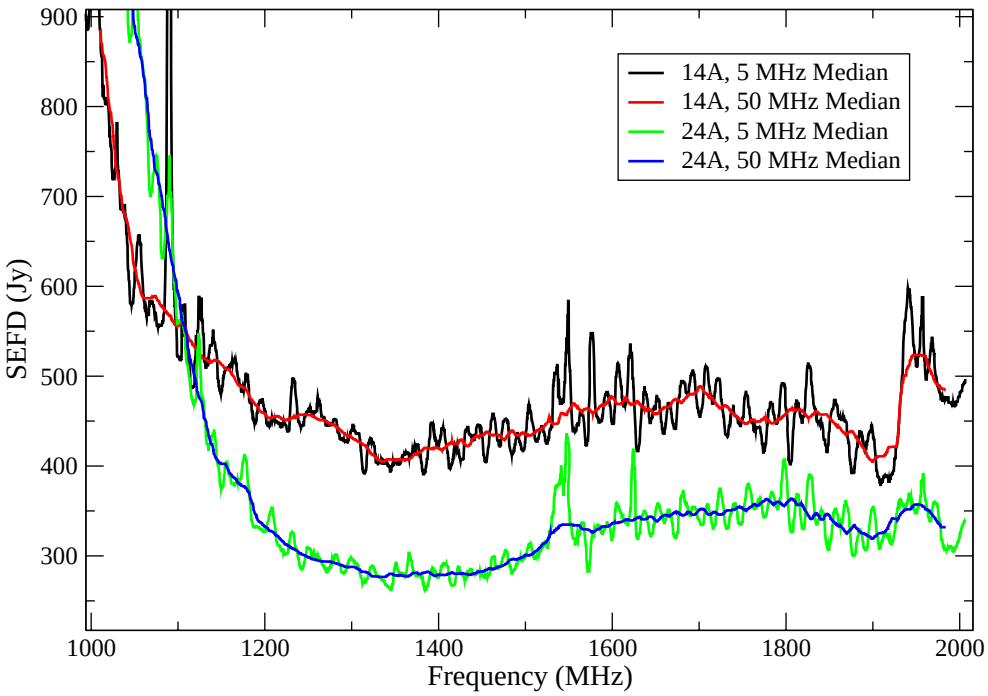

Figure 5: Showing the antenna sensitivity as functions of frequency for antennas 14 and 24. The improvement provided by the new OMT at low frequencies is clearly evident, as it shows only minor degradation in SEFD between 1300 and 1050 MHz. The general trend of a minimum near 1350 MHz, and a maximum near 1700 MHz agrees with calculation of feed performance made by S. Srikanth. The large spike in SEFD seen near 1090 MHz is due to a strong aeronautical radar.

It will be noted that the measured efficiency is the same for both RF and IF sampling – as expected, while the system temperature is increased by about 3K at all frequencies when the data passes through the IF system.

These results can be compared to the results for antenna 24 – the best EVLA antenna at L-band, as shown in Figure 7. We find that from these observations, antenna 24A has both a lower system temperature (by about 7K) and a higher antenna efficiency (by about 4%). The difference in efficiency is unexpected, and may reflect an error in the calibration of the efficiency. If so, the actual system temperature must be decreased in proportion (by about 3K), as the ratio is unaffected by calibration. Part of the difference in system temperature is accounted for by the new OMT, which adds about 5K more to the system temperature than the old OMT.

For both antennas, the same pattern in antenna efficiency is seen – a maximum near 1250 MHz, a minimum near 1600 MHz, and another maximum at 1900 MHz (or higher – the 'bump' referred to above, if an artifact, is perturbing the efficiency measurements). This general relation is seen in the performance simulations made by S. Srikanth, as reported in the EVLA FE Critical Design Review, although in that review, the low-frequency maximum is near 1400 MHz, and is considerably lower than that at 2000 MHz. However, these calculations used theoretical feed patterns, rather than measured far-field amplitude and phase patterns. Srikanth, Ruff, and Szpindor, in EVLA Memo #87 repeated these calculations, using actual measured illumination patterns at 1.4 and 2.0 GHz, including the effect of optimum subreflector position, to estimate efficiencies of 45% and 54% at these frequencies. The former value is very close to that observed, but the latter (2000 MHz) calculation is high by about 8%.

The overall efficiency of the EVLA L-band feed (42 to 46%) is lower than that for the VLA (50%) – a consequence of its size (about 30% smaller than the optimum) and the 2:1 Band Width

Ratio (BWR).

3.5 Focus and Sensitivity Dependencies on Elevation

The EVLA's L-Band feed was designed to minimize ground pickup at low elevations, and thus to avoid the strong elevation dependency of system sensitivity shown by the VLA's L-Band feed. Memo #85 showed that the new design indeed meets expectations, so that the EVLA will provide significantly better sensitivity than the VLA at low elevations – more than enough to offset the lower overall efficiency of the EVLA's feed. Here we extend this result to demonstrate that this excellent elevation performance extends over the whole band.

Sky dips were made on 15Dec2006, and power spectra taken at eleven elevations, approximately evenly spaced in $\sec(z)$. These data were calibrated in the manner previously described, and the excess system temperature above that measured at the zenith, for eleven frequencies across the band, are shown in Figure 8 for antennas 14A and 24A.

The figure shows that the rise in system temperature is very similar at all frequencies. There is good evidence that the ground pickup is greater at those frequencies where the efficiency is minimal, and vice versa. There is no evidence for an increase in ground pickup at very low frequencies. We confirm our result, shown in Memo #85, that the ground pickup by the EVLA feed is significantly better than that of the VLA's L-band feed.

A consequence of the compact wideband L-band horn design is that its focus position is a strong function of frequency – dropping by ∼57 cm between 1.0 and 2.0 GHz. The expected dependency of focus on frequency is non-uniform – nearly all the change occurs between 1.0 and 1.5 GHz. The range of travel required by the subreflector to offset this focus dependency is reduced by approximately the magnification – hence the subreflector position for maximum efficiency is expected to vary by approximately 7 cm.

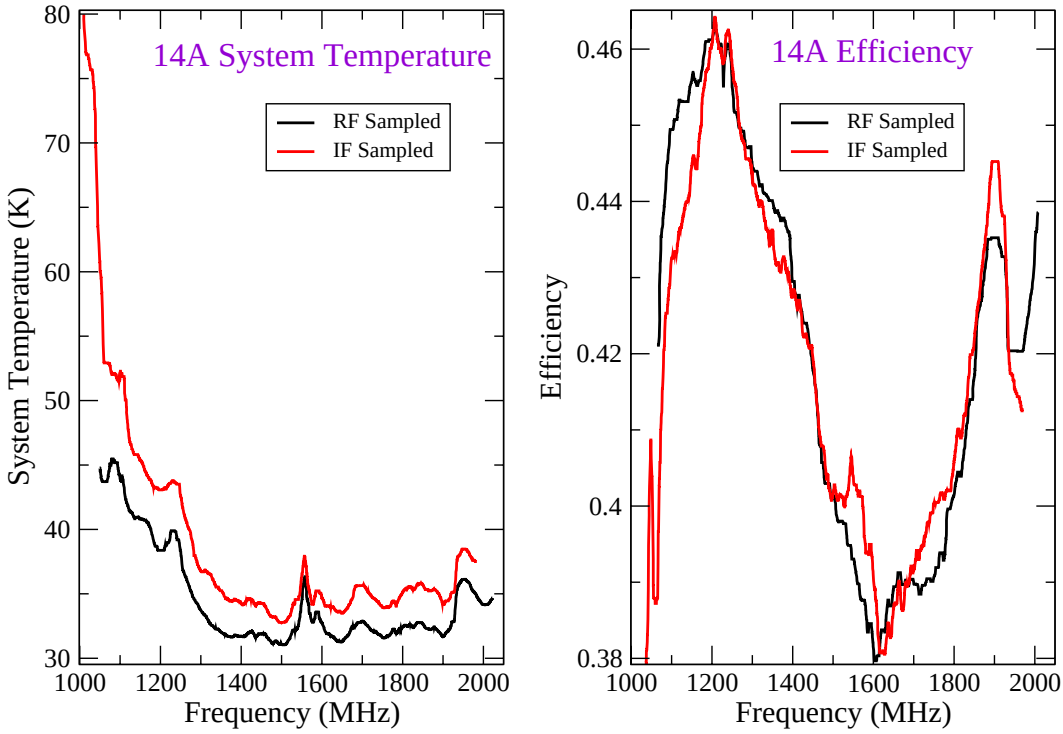

Figure 6: The cold-sky system temperature (left) and antenna efficiency (right) for antenna 14A. The IF system adds ∼3K to the system temperature.

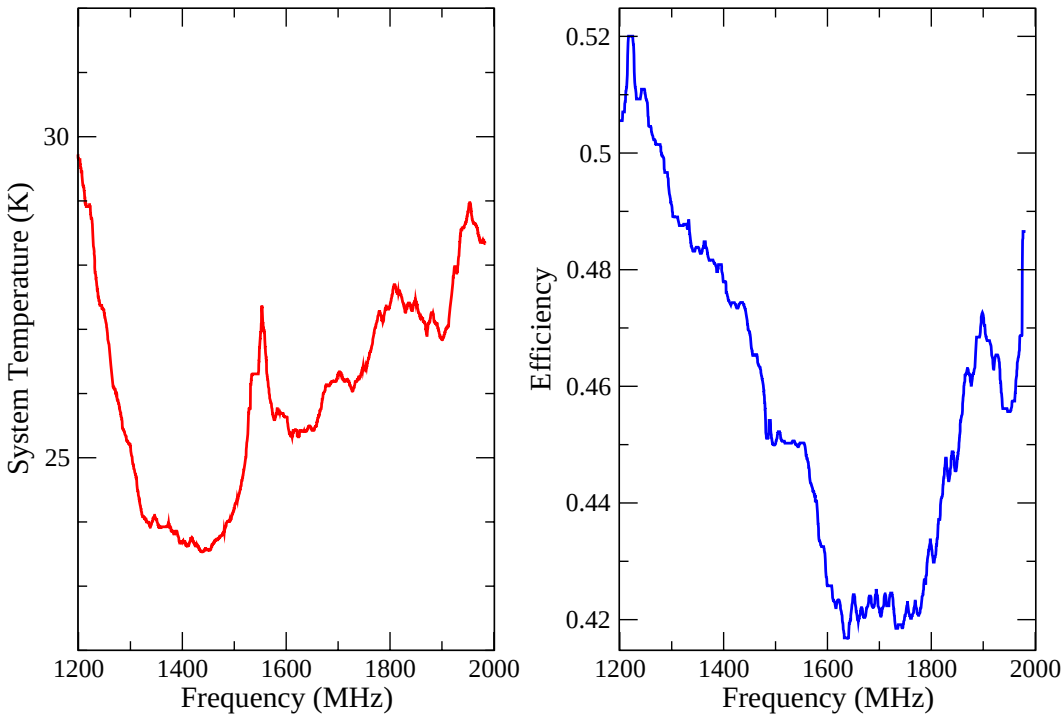

Figure 7: The cold-sky system temperature and antenna efficiency for antenna 24A, using IF sampling. Both the efficiency and system temperature are better than for antenna 14. The results below 1.2 GHz are not shown, as the VLA's OMT creates a very strong resonance below that frequency due to a waveguide resonance. the 'spike' near 1580 MHz is due to interference. Note that the scales in this figure are not the same as in Figure 6

We determined the dependency of system temperature and efficiency upon focus position by moving the subreflector over its full range while tracking Cygnus A, and taking snapshot spectra at nine positions, at 3cm intervals. The results are shown in Figure 9.

The expected behavior of efficiency on subreflector position is seen. The optimum position decreases with increasing frequency, by about 4 centimeters, with nearly all the change occuring between 1.0 and 1.5 GHz. Because the efficiency declines much more rapidly with subreflector position at higher frequencies, the optimum position of the subreflector for wide-band observations will be just above the optimum high-frequency position – at about ~ -5cm for 14A. At this position, the loss of efficiency at any frequency will be less than 2%. Also seen in this plot is the dependency of maximum efficiency with frequency – the curves peak at the highest values near 1200 MHz and 2000 MHz, and at the lowest values near 1600 MHz.

These results can be compared to the calculation of Srikanth et al., shown in Figure 25 of EVLA Memo #87. These calculations show the dependence on subreflector position to be much sharper than our observations – at 2 GHz, a 5-cm change in subreflector is calculated to decrease the efficiency by $\sim 23\%$, while we find the reduction over that range to be only $\sim 10\%$. Similarly, the change in optimum focus with frequency, between 1400 and 2000 MHz, in the calculations is expected to be about 3cm, while our observations show the change to be less than 1cm.

We also varied the focus position while observing blank sky at the zenith. No measureable effect was seen, indicating negligible additional ground pickup due to defocussing. The effect of defocussing is to broaden the main beam, and hence lower forward efficiency.

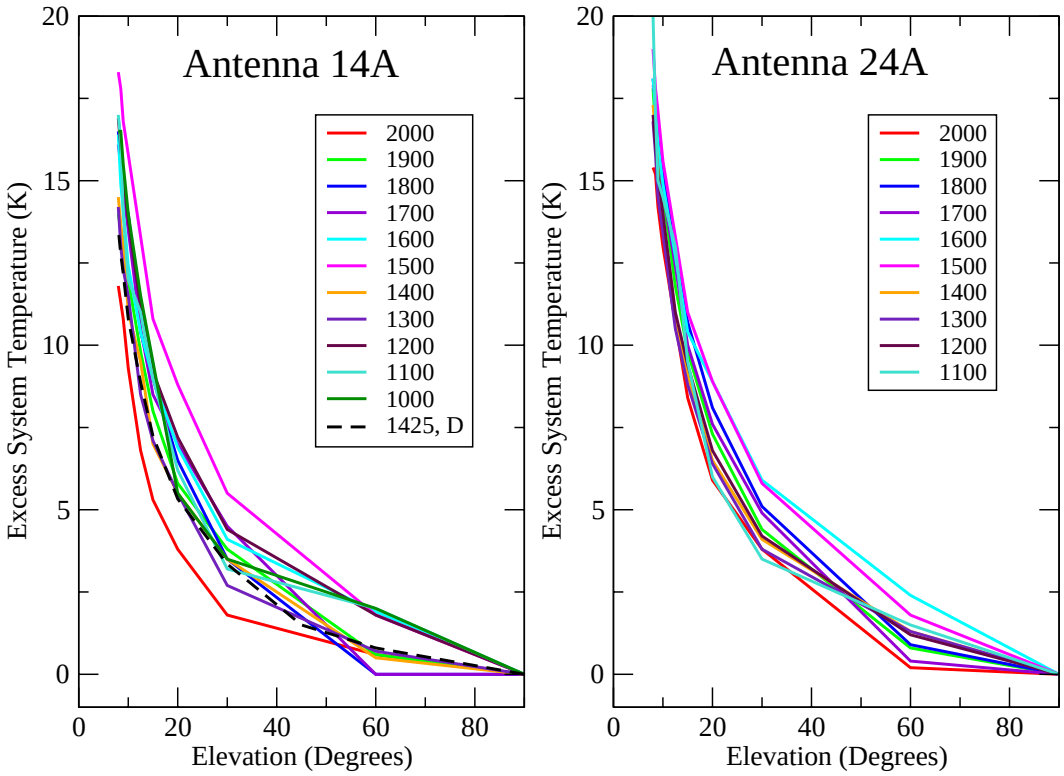

Figure 8: The additional system temperature as a function of elevation and frequency, for antennas 14A and 24A. The majority of this increase is caused by ground pickup. The dashed line in the left panel shows the results using 'direct' RF sampling.

4 Future Tests

We list here some remaining issues which will require future tests.

- Polarimetric observations, as a function of frequency, need to be made to measure the amplitude and stabilitiy of the cross-polarization response. These are best done after a second new design OMT is installed.
- Our present tests indicate the IF electronics is adding ∼3 K to the system temperature – considerably more than our models. System temperature measures of antenna 24, before and after the IF should tell us if the addition in antenna 14 is due to a peculiarity in that antenna.
- Our observations on antenna 14 – which is wide-open to the aeronautical navigation bands – shows there is no obvious degradation in performance due to these emission. Further and more extensive studies are needed, particularly when we have four or more antennas outfitted with the new OMTs, and the prototype WIDAR correlator is in place.
- The test OMT on antenna 14 is known to add about 5K over the old model OMTs. Ongoing improvements in subsequent models should decrease this addition. This should be reflected in better performance on the sky.

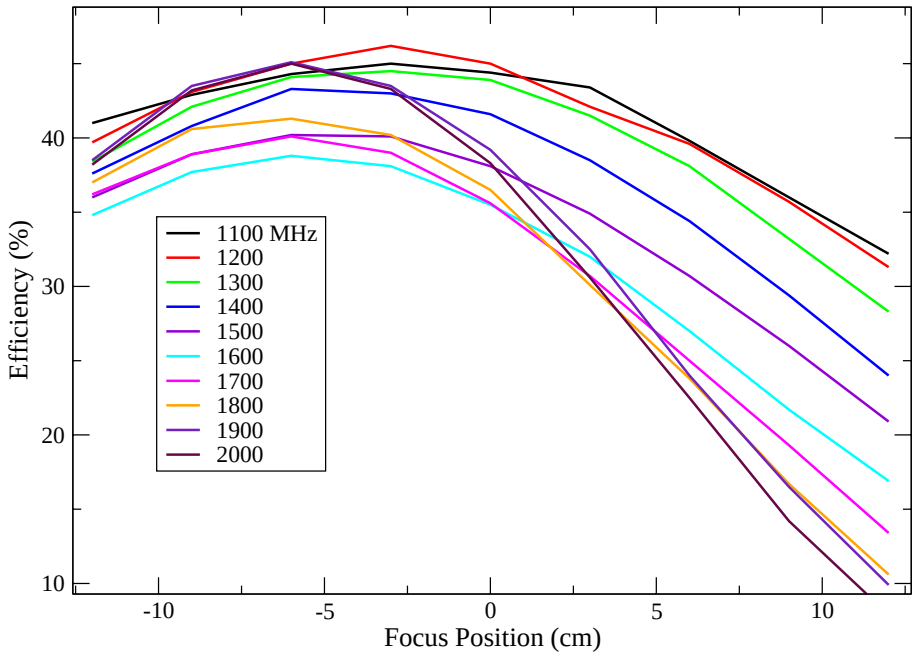

Figure 9: The efficiency of antenna 14A as a function of subreflector position, for the frequencies shown. The optimum position varies by about 4 cm over the full frequency range, with most of the variation seen within the lower half of the frequency range. At the optimum position of ~ -5 cm, the loss of efficiency at all frequencies is less than 2%.